International Journal of Scientific Research and Engineering Development-– Volume 9 Issue 3, May-June 2026
Available at www.ijsred.com

RESEARCH ARTICLE OPEN ACCESS

Dual-Band Rasorber With Two Transmission Windows and Three Absorption Bands for A/T/A/T/A Spectral Response

Kasun Athapatthu*, Li Chen**
*(School of Electronics and Information Engineering, Nanjing University of Information Science and Technology, Nanjing, China
Email: athapatthukasun@gmail.com)
** (School of Electronics and Information Engineering, Southwest Petroleum University, Chengdu, China
Email:lic44799@gmail.com)

--************************----------------------------------

Abstract:
This paper presents a dual-band rasorber exhibiting two transmission windows and three absorption states (A/T/A/T/A) in the microwave frequency range. The proposed structure consists of a two-layer metasurface configuration comprising a patterned lossy layer and a complementary lossless layer, enabling controlled multi-band spectral response. The lossy layer employs a four-fold symmetric arrangement of coupled rectangular resonators integrated with multi-branch dipole elements and lumped resistors, supporting both absorption and transmission resonances. The lossless layer is designed to introduce two corresponding transmission bands that align with those of the lossy layer, enabling efficient energy tunneling at the desired frequencies. The rasorber demonstrates three absorption bands at 4.6–5.3 GHz, 6.58–8.32 GHz, and 11.15–12.17 GHz, along with two transmission windows at 5.98–6.38 GHz and 9.1–9.85 GHz, both exhibiting with very low insertion loss. Additionally, stable performance is maintained under oblique incidence up to 30°, making it suitable for stealth radome and advanced electromagnetic filtering applications.
Keywords — **Rasorber, Frequency-selective surface (FSS), Metasurface, Dual-band transmission, Electromagnetic absorber, Angular stability, Stealth radome**

--************************----------------------------------

I. Introduction

Electromagnetic absorbers and frequency-selective surfaces (FSS) are fundamental components in radar cross-section (RCS) reduction, electromagnetic compatibility, and stealth radome applications [1]–[4]. Classical absorber configurations such as the Salisbury screen and Jaumann absorber demonstrated high absorption through resistive loading and quarter-wavelength spacing [3], [4], but inherently lack spectral selectivity. In contrast, FSS structures enable frequency-dependent transmission and reflection control [2], yet cannot dissipate incident energy. To address the growing demand for simultaneous absorption and transmission within a single aperture, hybrid metasurface structures known as rasorbers have been introduced, combining resistive and reactive elements to achieve integrated spectral filtering and absorption [5]–[8]. By embedding lumped resistors into periodic resonators, controlled absorption bands can be engineered, while complementary lossless layers enable selective transmission windows [9]–[12].

Recent studies have explored multi-state rasorbers with improved functionality. For instance, Shang et al. [5] proposed a resistive–reactive rasorber exhibiting a three-state A/T/A response, though with limited angular stability. Chen et al. [13] demonstrated a dual-band rasorber with two transmission windows, but the reported insertion loss exceeded 3 dB and angular performance was not extensively validated. More recently, Li et al. [14] and Yi et al. [15] developed polarization and

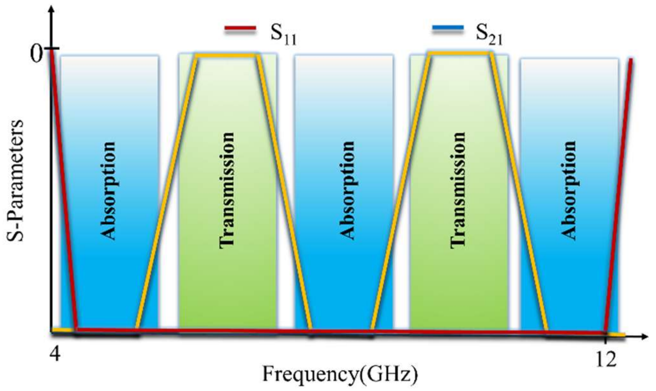

Figure 1: Behaviour of the Proposed Design

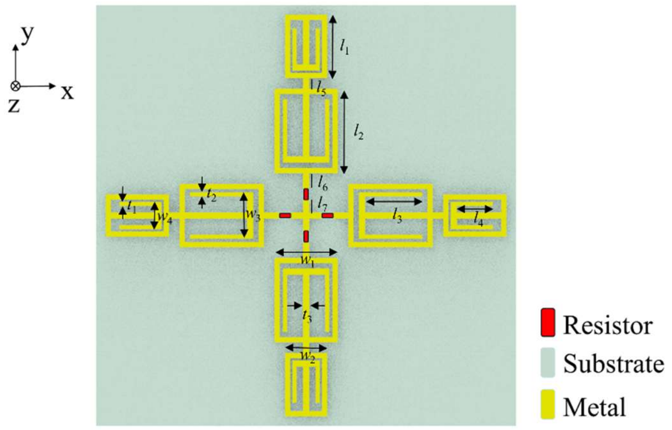

Figure 2: Unit Cell of the Lossy Layer (Parameters: l_1 = 3mm, l_2 = 4mm, l_3 = 3mm, l_4 = 2mm, l_5 = 1mm, l_6 = 0.8mm, l_7 = 0.8mm, w_1 =, w_1 = 3mm, w_2 = 2mm, w_3 = 1.3mm, w_4 = 2mm, t_1 = 0.2mm, t_2 = 0.2mm, t_3 = 0.3mm)

angularly stable rasorbers, respectively; however, these designs were largely restricted to single transmission windows or did not simultaneously achieve low insertion loss and multi-band absorption. Consequently, realizing a compact rasorber with a full A/T/A/T/A response, low-loss transmission, and stable oblique performance remains a significant challenge [16]–[18].

In this work as shown in Figure 1, a dual-band rasorber with a five-state A/T/A/T/A response is proposed. The structure employs a cascaded metasurface configuration consisting of a patterned lossy layer and a complementary lossless layer. The lossy layer integrates four-fold symmetric nested rectangular resonators with multi-branch dipole elements and lumped resistors, supporting both

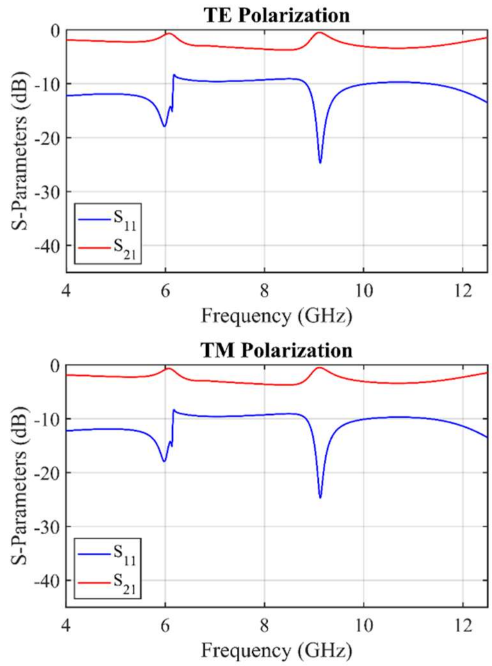

Figure 3: S-Parameters of the Lossy Layer

absorption and transmission resonances. The lossless layer introduces two corresponding transmission bands aligned with those of the lossy layer, enabling efficient dual-passband operation. The proposed design achieves three absorption bands (4.6–5.3 GHz, 6.58–8.32 GHz, and 11.15–12.17 GHz) and two transmission windows (5.98–6.38 GHz and 9.1–9.85 GHz) with insertion loss below 3 dB. Furthermore, stable performance is maintained up to 30° oblique incidence, making the structure suitable for advanced stealth radome and electromagnetic filtering applications.

II. Design and Analysis

The objective of this work is to realise a compact rasorber exhibiting two transmission windows and three absorption bands (A/T/A/T/A response) with low insertion loss and stable angular performance. To achieve this, a cascaded metasurface configuration is employed, consisting of a resistively loaded lossy layer and a complementary lossless layer separated by an air spacer. The lossy layer is engineered to simultaneously support dual

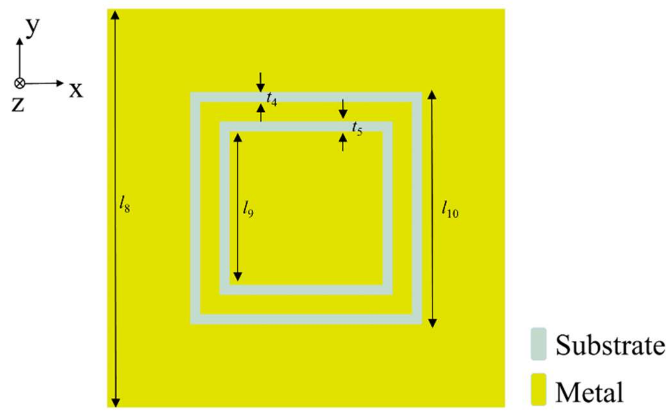

Figure 4: Unit Cell of the Lossless Layer (Parameters: l_8 = 20mm, l_9 = 8.7mm, l_{10} = 11.65mm, t_4 = 1mm, t_5 = 1mm)

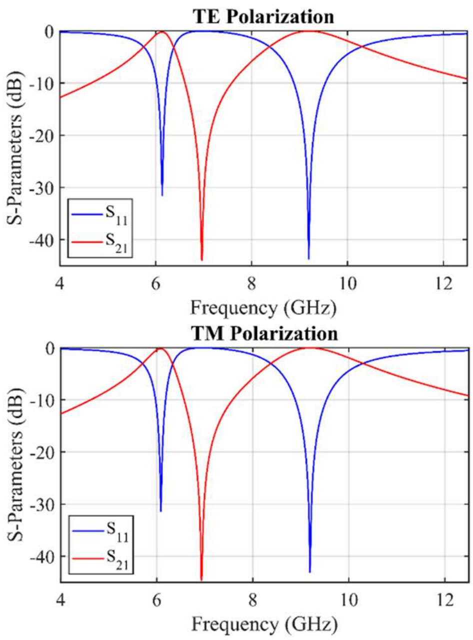

Figure 5: S-Parameters of the Lossless Layer

transmission windows and out-of-band absorption, while the lossless layer reinforces the transmission response at the desired frequencies.

A. Lossy Layer

The lossy layer is designed using a four-fold symmetric unit cell to ensure polarization-insensitive operation. It consists of two nested rectangular resonators integrated with multi-branch (E-shaped) dipole elements and resistive loading. The two resonators are responsible for distinct

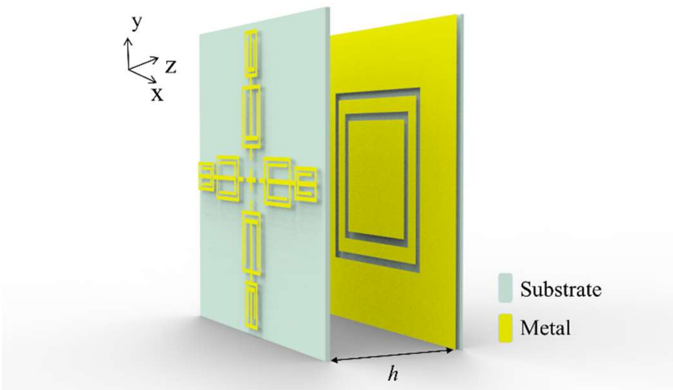

Figure 6: Cell Structure of the Proposed Rasorber h = 9mm

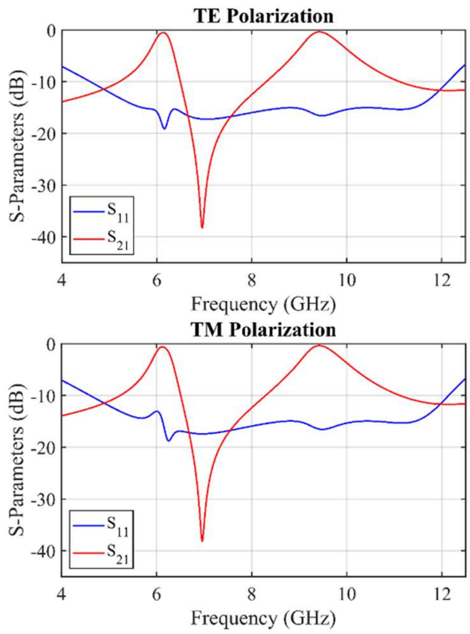

Figure 7: Performance of the Proposed Rasorber

frequency responses, where the smaller structure controls the higher-frequency region and the larger structure governs the lower-frequency region.

Unlike conventional absorptive surfaces, the proposed lossy layer supports both transmission and absorption. Specifically, it exhibits two intrinsic transmission windows associated with resonant current distributions in the embedded dipole structures, while strong absorption occurs outside these bands due to resistive dissipation. The placement of lumped resistors along the central current paths ensures efficient energy absorption at non-transmitting frequencies without suppressing

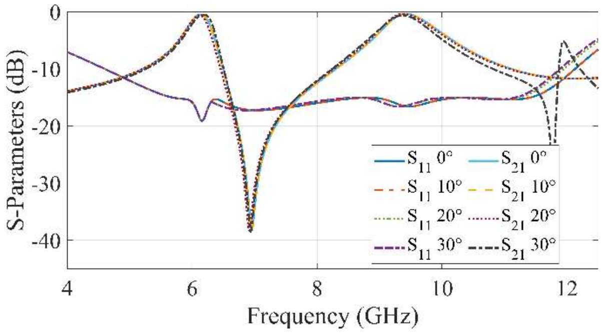

Figure 8: Angular Stability of the Proposed Rasorber

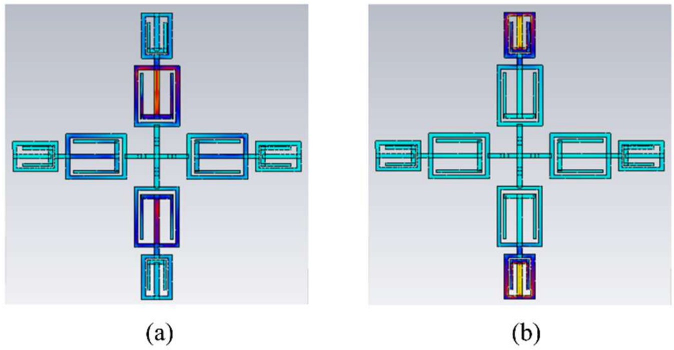

Figure 9: Surface Currents

the desired transmission resonances. The unit cell geometry and corresponding TE/TM responses are shown in Figure 2 and Figure 3, demonstrating polarization-insensitive dual-band transmission with out-of-band absorption.

B. Lossless Layer

The lossless layer is realised as a slotted metallic surface forming a complementary frequency-selective structure. It consists of two concentric square slot apertures designed to resonate at the same frequencies as the transmission windows of the lossy layer. According to Babinet's principle, these slot elements produce bandpass responses with high transmission efficiency.

The larger slot corresponds to the lower transmission band, while the smaller slot produces the higher-frequency transmission window. Since no resistive elements are included, the transmission peaks exhibit low insertion loss and sharp selectivity. The unit cell configuration and TE/TM responses are illustrated in Figure 4 and Figure 5, confirming stable dual-band transmission behavior.

II. Simulation results and Analysis

The geometry of the proposed rasorber is shown in Figure 6. The structure consists of a cascaded two-layer metasurface configuration comprising a resistively loaded lossy layer and a complementary lossless layer separated by a 9 mm air gap. The lossy layer employs nested rectangular resonators integrated with multi-branch dipole elements and lumped resistors, while the lossless layer consists of two concentric square slot apertures designed to support dual transmission resonances. Full-wave simulations were performed in CST Microwave Studio using periodic boundary conditions and Floquet port excitation.

Figure 7 presents the simulated transmission and ((|S21|) reflection (|S11|) responses under normal TE and TM incidence. The proposed structure exhibits a clear five-state A/T/A/T/A response with three absorption bands at 4.6–5.3 GHz, 6.58–8.32 GHz, and 11.15–12.17 GHz, together with two transmission windows located at 5.98–6.38 GHz and 9.1–9.85 GHz. Both transmission bands maintain insertion loss below 3 dB. The close agreement between the TE and TM responses confirms the polarization-insensitive characteristic of the proposed design, which is achieved through the four-fold symmetric unit cell configuration.

The angular stability of the rasorber is evaluated in Figure 8 for TE and TM polarisations under oblique incidence angles from 0° to 30°. The proposed structure preserves its overall spectral response with only minor frequency variations as the incident angle increases, demonstrating stable operation suitable for practical stealth and filtering

To further investigate the operating mechanism, the surface current distributions at the two transmission windows are illustrated in Figure 9. At the lower transmission band, the dominant currents are concentrated on the larger resonator and corresponding larger slot aperture, whereas the upper transmission band is mainly governed by the smaller resonator and smaller slot structure. These results confirm that the two transmission windows

Comparison Table

Reference	Response Type	Absorption Bands	Transmission Windows	Insertion Loss(dB)	Angular Stability	Polarization
[5]	A/T/A	4.8–5.5 GHz, 9.0–13.5 GHz	7.0–8.5 GHz	< 3	Up to 30°	Dual-polarized
[6]	A/T/A	3.2–5.5 GHz, 7.2–14.6 GHz	5.6–7.0 GHz	< 3	-	Dual-polarized
[9]	A/T/A/T/A	4.1–7.5, 9.1–12.3, 14.0–19.7 GHz	8.5 GHz & 13.0 GHz	< 2	-	Dual-polarized
[14]	A/T/A	4.0–5.5 GHz, 7.5–12.0 GHz	5.9–7.0 GHz	< 2	Up to 30°	Polarization-insensitive
[15]	A/T/A/T	3.7–10.5 GHz, 12.6–14.6 GHz	10.7 GHz & 16.0 GHz	< 2	Up to 20°	Polarization-insensitive
This Work	**A/T/A/T/A**	**4.6–5.3, 6.58–8.32, 11.15–12.17 GHz**	**5.98–6.38 & 9.1–9.85 GHz**	**< 1**	**Up to 30°**	**Polarization-insensitive**

are independently controlled by resonators with different electrical lengths, while the resistively loaded regions contribute to out-of-band absorption.applications.

References

[1] R. L. Fante and M. T. McCormack, "Reflection properties of the Salisbury screen," *IEEE Trans. Antennas Propag.*, vol. 36, no. 10, pp. 1443–1454, Oct. 1988.
[2] B. A. Munk, *Frequency Selective Surfaces: Theory and Design*. New York: Wiley, 2000.
[3] F. Costa and A. Monorchio, "A frequency selective radome with wideband absorbing properties," *IEEE Trans. Antennas Propag.*, vol. 60, no. 6, pp. 2740–2747, Jun. 2012.
[4] B. A. Munk, P. Munk, and J. Pryor, "On designing Jaumann and circuit analog absorbers (CA absorbers) for oblique angle of incidence," *IEEE Trans. Antennas Propag.*, vol. 55, no. 1, pp. 186–193, Jan. 2007.
[5] Y. Shang, Z. Shen, and S. Xiao, "Frequency-selective rasorber based on square-loop and cross-dipole arrays," *IEEE Trans. Antennas Propag.*, vol. 62, no. 11, pp. 5581–5589, Nov. 2014.
[6] Q. Chen, D. Sang, M. Guo, and Y. Fu, "Frequency-selective rasorber with interabsorption band transparent window and interdigital resonator," *IEEE Trans. Antennas Propag.*, vol. 66, no. 8, pp. 4105–4114, Aug. 2018.
[7] H. Huang, C. Hua, and Z. Shen, "Absorptive frequency-selective transmission structures based on hybrid FSS and absorber," *IEEE Trans. Antennas Propag.*, vol. 70, no. 8, pp. 5606–5613, Aug. 2022.
[8] Q. Zhou, M. Guo, H. Moghadas, Z. Wu, P. Liu, and M. Daneshmand, "A frequency selective rasorber with three transmission bands and three absorption bands," *IEEE Access*, vol. 7, pp. 160973–160981, Nov. 2019.
[9] N. Liu, X. Sheng, and X. Zhao, "Design of dual-polarized frequency selective rasorber with two independent transmission windows using multi-resonators," *IEEE Access*, vol. 8, pp. 223723–223729, Dec. 2020.
[10] M. Guo, M. Chen, Q. Bai, T. Wei, and Y. Fu, "Wide transmission band frequency-selective rasorber based on convoluted resonator," *IEEE Antennas Wireless Propag. Lett.*, vol. 19, no. 5, pp. 846–850, May 2020.
[11] M. Guo, Q. Chen, Z. Sun, D. Sang, and Y. Fu, "Design of dual-band frequency-selective rasorber," *IEEE Antennas Wireless Propag. Lett.*, vol. 18, no. 5, pp. 841–845, May 2019.
[12] X. Xiu, W. Che, Y. Han, and W. Yang, "Low-profile dual-polarization frequency-selective rasorbers based on simple-structure lossy cross-frame elements," *IEEE Antennas Wireless Propag. Lett.*, vol. 17, no. 6, pp. 1002–1005, Jun. 2018.
[13] Q. Chen, S. Yang, J. Bai, and Y. Fu, "Design of absorptive/transmissive frequency-selective surface based on parallel resonance," *IEEE Trans. Antennas Propag.*, vol. 65, no. 9, pp. 4897–4902, Sep. 2017.
[14] Y. Li, P. Ren, Z. Xiang, and B. Xu, "Design of miniaturized frequency-selective rasorber with embedded dual-bow resonators," *IEEE Antennas Wireless Propag. Lett.*, vol. 22, no. 2, pp. 442–446, Feb. 2023.
[15] M. M. Zargar, A. Rajput, K. Saurav, and S. K. Koul, "Miniaturized design of dual transmission frequency selective rasorber with wide angular stability," *IEEE Open J. Antennas Propag.*, vol. 5, pp. 922–932, 2024.
[16] M. M. Zargar, A. Rajput, K. Saurav, and S. K. Koul, "Polarization-insensitive frequency selective rasorber with broad absorption band and two-sided transmission bands," *Int. J. RF Microw. Comput.-Aided Eng.*, vol. 32, no. 3, Art. no. e23067, 2022.
[17] Z. Shen, J. Wang, and B. Li, "3-D frequency selective rasorber: Concept, analysis, and design," *IEEE Trans. Microw. Theory Techn.*, vol. 64, no. 10, pp. 3087–3096, Oct. 2016.
[18] B. Li and Z. Shen, "Wideband 3D frequency selective rasorber," *IEEE Trans. Antennas Propag.*, vol. 62, no. 12, pp. 6536–6541, Dec. 2014.